

Numerical Analysis of Flow in the Gap between a Simplified Tractor-Trailer Model and Cross Vortex Trap Device

Terrance Charles, Zhiyin Yang, Yiling Lu

Abstract—Heavy trucks are aerodynamically inefficient due to their un-streamlined body shapes, leading to more than of 60% engine power being required to overcome the aerodynamics drag at 60 m/hr. There are many aerodynamics drag reduction devices developed and this paper presents a study on a drag reduction device called Cross Vortex Trap Device (CVTD) deployed in the gap between the tractor and the trailer of a simplified tractor-trailer model. Numerical simulations have been carried out at Reynolds number 0.51×10^6 based on inlet flow velocity and height of the trailer using the Reynolds-Averaged Navier-Stokes (RANS) approach. Three different configurations of CVTD have been studied, ranging from single to three slabs, equally spaced on the front face of the trailer. Flow field around three different configurations of trap device have been analysed and presented. The results show that a maximum of 12.25% drag reduction can be achieved when a triple vortex trap device is used. Detailed flow field analysis along with pressure contours are presented to elucidate the drag reduction mechanisms of CVTD and why the triple vortex trap configuration produces the maximum drag reduction among the three configurations tested.

Keywords—Aerodynamic drag, cross vortex trap device, truck, RANS.

I. INTRODUCTION

THE aerodynamics of trucks is an area in which better understanding, and improvements can be made despite major achievements in the past years [1], [2]. There are several aerodynamic forces acting on a driving vehicle, which directly affect the operation of a vehicle [3]. Aerodynamic loads on the vehicle may act in different ways but primarily result in drag being generated which affect the acceleration and velocity of a vehicle etc., and ultimately leading to fuel consumption efficiency.

Generally speaking, pressure drag makes up most of the total drag force experienced by a truck with the surface friction drag contributing to a miniscule amount of the overall drag. Pressure drag reduction of a truck can be achieved mainly in three areas: the front part of the tractor, rear part of the trailer and the gap between the tractor and trailer [4]. The gap between the tractor and trailer has a significant effect on the total drag force and a better understanding of the flow field

in the gap is needed for drag reduction in this region [5].

One simple, yet effective drag reduction device which has been used in the tractor and trailer gap is CVTD [6]. CVTD are equally spaced vertical slabs that extend perpendicular from the front face of the trailer. The primary aim of these devices is to trap vortices and stabilize the flow in the gap between the tractor and trailer. Kumar [7] analyzed a similar CVTD design along with Coanda device mounted to the leading edge corners of the trailer in the gap. Analysis carried out without any devices in the gap showed a combination of uneven high and low-pressure contours in the gap between tractor and trailer. When the model was tested with CVTD installed, pressure contours on the front face of the trailer had a better and even pressure distribution which was primarily due to vortices being stabilized by the use of CVTD [8].

Despite a significant amount of drag being generated in the tractor and trailer gap region, the research on the drag reduction in the gap region is scarce in literature. The present work investigates the effectiveness of a three CVTD configurations using a simplified tractor-trailer model [9] as shown in Fig. 1. The model consists of a front box which represents the tractor and a rear box representing trailer and is connected by two cylinders. The model dimensions are the same as used in the experiment [9] and the Reynolds number based on inlet velocity and height of the trailer box is $Re = 0.51 \times 10^6$. The oncoming free stream velocity is at 0° yaw angle, which is in no cross wind condition.

Figs. 2-4 show the three CVTD configurations used in the present study. Case 1 is a single vortex trap device or commonly called as a gap splitter. The vertical slab is mounted on the front face along the mid plane of the trailer. Case 2 is a dual vortex trap device which is aligned with the midpoint of the two connecting cylinders and case 3 is a triple vortex trap device which is a combination of case 1 and case 2. The cross-vortex trap devices extend $0.085b$ from the front face of the trailer (b is the height of the trailer and equals 0.305 m). The height of the device is of the same height as the trailer and each slab's width/thickness of the device is 0.01 m.

II. NUMERICAL METHODS AND COMPUTATIONAL DETAILS

The governing equations are solved numerically using a finite volume method and the computer code used is STAR CCM+. The second-order upwind scheme is employed for spatial discretization. Fig. 5 shows a 2D view of the mesh. The mesh is refined in the region surrounding the truck as shown in the figure and a two layer all wall y^+ approach is used for

T. Charles is Ph.D. student in the College of Engineering and Technology, University of Derby, Derby, UK (corresponding author, phone: 07448435903; e-mail: t.charles@derby.ac.uk)

Z. Yang is in the College of Engineering and Technology, University of Derby, Derby, UK (e-mail: z.yang@derby.ac.uk).

Y.Lu is a senior lecturer in the College of Engineering and Technology, University of Derby, Derby, UK (e-mail: y.lu@derby.ac.uk).

all the walls in the simulations. In terms of boundary conditions, a viscous wall (no-slip) boundary condition is applied on the top and lateral walls. A uniform inlet velocity, $U_\infty = 24.4$ m/s, is set at the inlet which is the same used in the wind tunnel tests. No value for turbulence intensity was reported in the wind tunnel experiments [9] and in the numerical simulation [10]. On the lower wall the velocity component in the stream wise direction is set equal to the inlet velocity, matching the moving ground condition in the experiment.

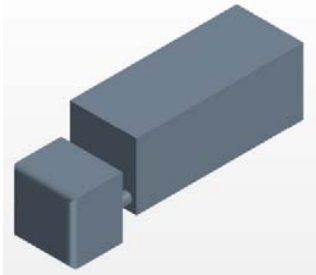


Fig. 1 Generic Test Case

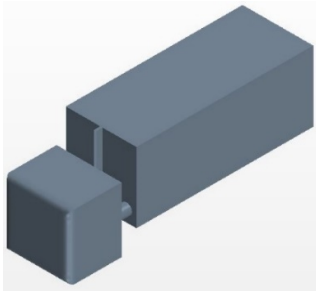


Fig. 2 Case 1

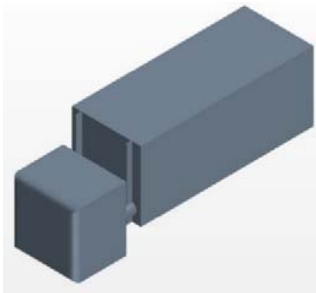


Fig. 3 Case 2

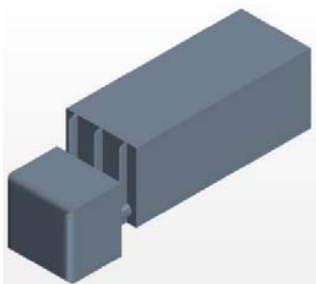


Fig. 4 Case 3

A grid independence study was carried out with three different meshes, coarse mesh of 4M cells, medium mesh of 5.8M cells and fine mesh of 8.0M cells. Fig. 6 presents axial velocity profile on the XY plane (located half way in the Z direction) at $x = 1.13$ m downstream from the front face. It can be seen from the figure that the results obtained using the coarse mesh are different from those obtained using the medium and fine meshes. However, the results obtained using the medium mesh are more or less the same as those obtained using the fine mesh, suggesting that the grid independent results have been achieved. Hence there is no need to refine the mesh further and the fine mesh has been used in the present study.

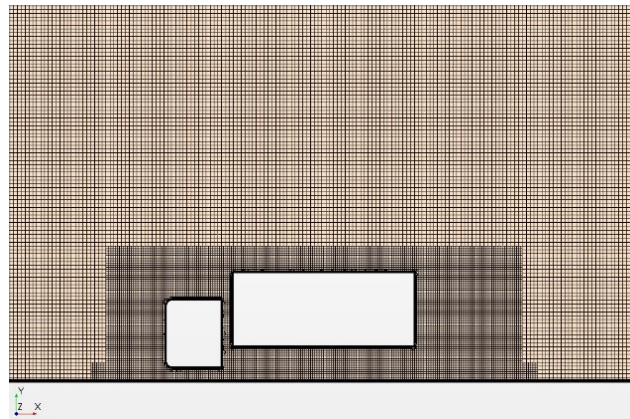


Fig. 5 A 2D view of the mesh around the truck

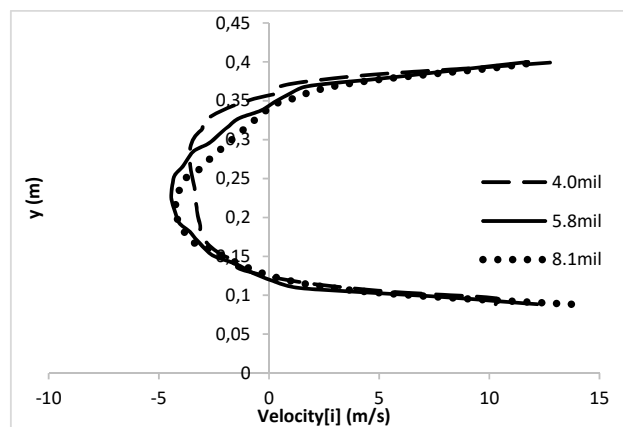


Fig. 6 Velocity profile obtained using three meshes

Choosing an appropriate turbulence model is always difficult as there is not any recognized best turbulence model since their performances vary depending on the flow situations. In the present study three well regarded and widely used turbulence models were assessed and Table I shows the drag coefficient obtained from those turbulence model and the experimental data [9]. It can be seen that SST $k - \omega$ model produces the best results in this flow situation and hence it has been selected in the present study.

TABLE I
PREDICTED DRAG COEFFICIENT AND THE EXPERIMENTAL RESULTS

	C_d	ΔC_d
Experiment [9]	0.77	
Realizable $k - \epsilon$	0.862	11.95%
SST $k - \omega$	0.809	5.06%
RSM	0.820	6.49%

III. RESULTS AND ANALYSIS

To facilitate comparison, simulation was first carried out without CVTD and Fig. 7 presents the streamlines on the XY plane located half way in the span wise direction. The flow impinges on the front face of the tractor and top part of the trailer front face, resulting in two high pressure regions as shown in Fig. 8. The flow separates at the leading edges of the tractor. Part of the flow enters the gap and remaining part of the flow moves along the top surface of the trailer. Another separation bubble forms on the top of the trailer.

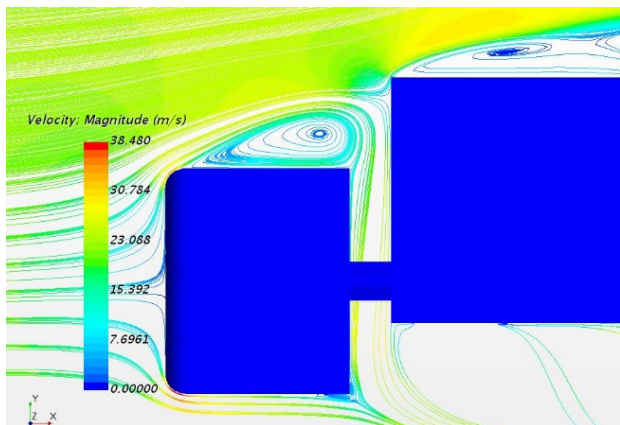


Fig. 7 Streamline view in the XY plane at $Z = 0$

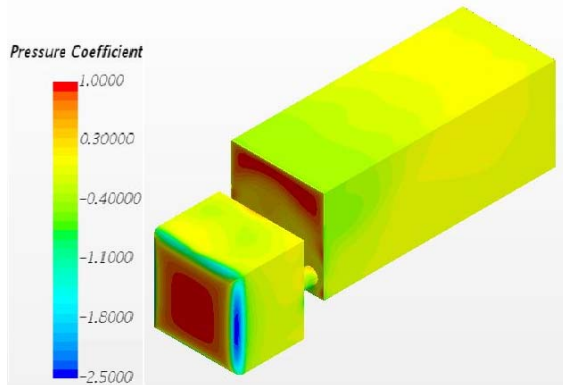


Fig. 8 Pressure coefficient contour

Fig. 9 shows velocity vectors on the XZ plane at $y = 0.02$ m and it can be seen that two large vortices form at the two corners in the gap. However, the flow field has been significantly altered when CVTD is mounted on the front face of the trailer as shown in Figs. 10 (a)-(c). One obvious difference is that for all three cases the two large corner vortices formed without CVTD disappear and several

relatively smaller vortices can be observed in the gap. For case 1, three vortices are clearly observable and about 5 vortices seem to form for case 2 but three of those vortices are not apparent, indicating that those three vortices are not that strong. Interestingly for case 3, similar to case 1, there are also three clearly observable vortices but it can be seen that they are stronger than those in case 1.

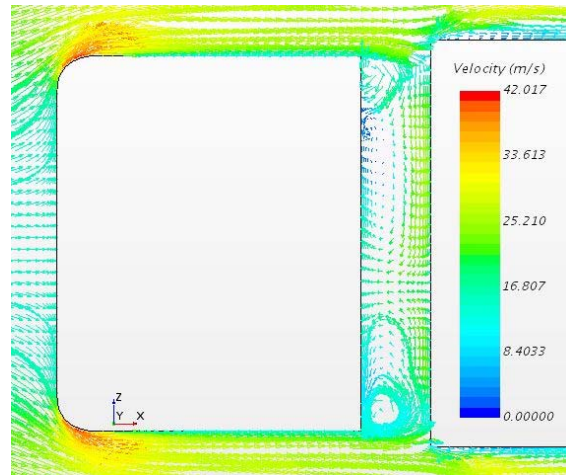
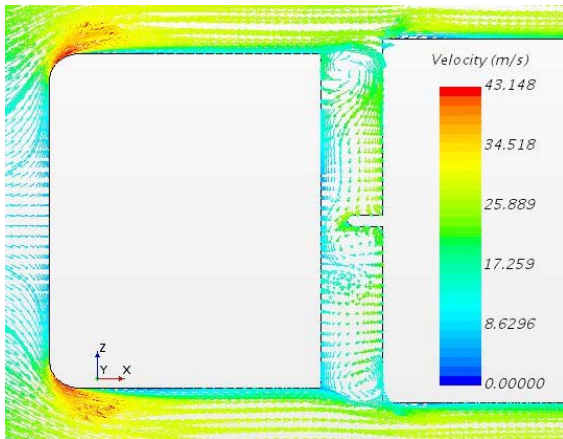


Fig. 9 Velocity vector in the gap on the XZ plane at $y = 0.20$ m

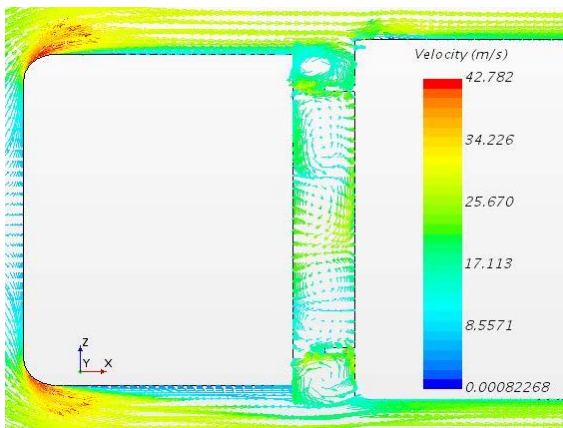
The predicted drag coefficients for the three cases are compared against the case without CVTD (base case) as shown in Table II. It is evident that the most drag reduction, 14.7%, is obtained for case 3 while for cases 1 and 6 similar amount of drag reduction, about 10%, is achieved. Hence among the three cases tested, case 3 with three triple vortex trap devices mounted on the front face of the trailer proves to be the most efficient arrangement. This indicates that a lower pressure distribution on the front face of the trailer for case 3, which is due to stronger vortices generated as shown in Fig. 10 (c). This can be confirmed from contours of pressure coefficient on the front surface of the trailer as shown in Figs. 11 (a)-(c). It can be seen that more uniform and slightly lower pressure regions are observed for case 3, leading to larger drag reduction.

TABLE II
COEFFICIENT OF DRAG COMPARISON AGAINST THE BASE CASE WITHOUT CVTD

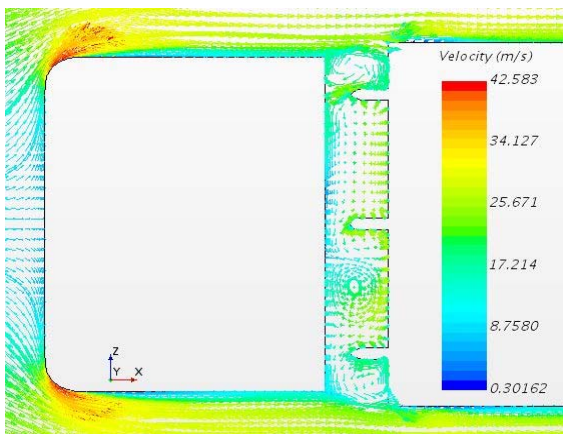
	C_d	Percentage reduction in C_d
Base case	0.809	
Case 1	0.723	10.6%
Case 2	0.728	10%
Case 3	0.690	14.7%



(a) Case 1

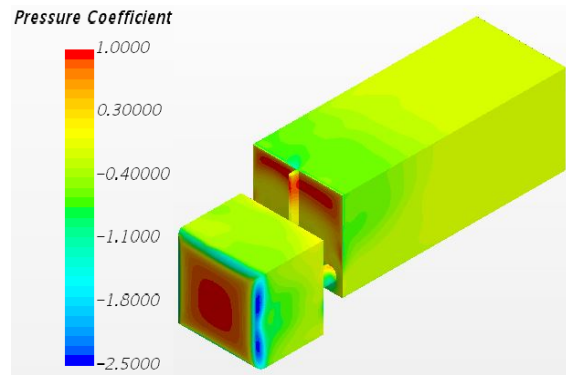


(b) Case 2

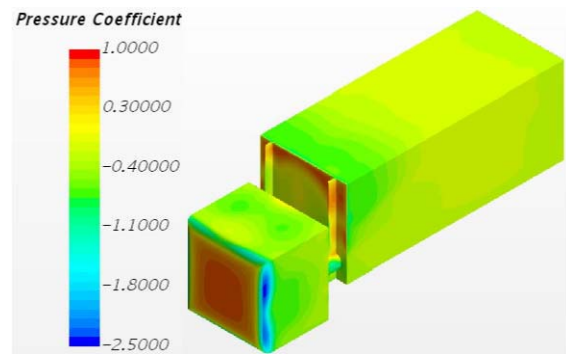


(c) Case 3

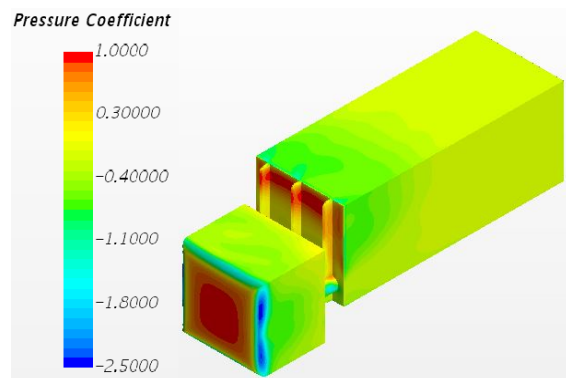
Fig. 10 Velocity vectors in the gap on the XZ plane at $y = 0.20$ m: (a) single vortex trap device, (b) double vortex trap device, (c) triple vortex trap device



(a) Case 1



(b) Case 2



(c) Case 3

Fig. 11 Contours of pressure coefficient. (a) Case 1, (b) Case 2, (c) Case 3

IV. CONCLUSION

A numerical study of the flow over a simplified tractor-trailer geometry with three configurations of CVTD installed in the gap between the tractor and trailer has been carried out using the RANS approach. The main findings from the present study are:

- 1) Among the three turbulence models assessed in the present study the SST $k-\omega$ turbulence model has produced the closest result to the experimental data.
- 2) The RANS approach with a suitable turbulence model can

produce accurate results in terms of global parameters such as the drag coefficient (5.06% difference between the prediction and experimental data) for such complicated flows in the present study.

- 3) It is demonstrated that CVTD is a simple and yet effective drag reduction device as the drag has been reduced considerably with all three configurations of CVTD, and case 3 with a triple vortex trap device proves to be the most effective one achieving about 15% of drag reduction.
- 4) The drag reduction mechanism is mainly due to the generation of strong vortices in the gap region, leading to lower pressure on the front surface of the trailer.

REFERENCES

- [1] K.R. Cooper, "National Research Council of Canada," Springer Link, vol. 19 pp.9-28, 2004.
- [2] D. L. W. K. C. Ilhan Bayraktar, "An Assessment of drag reduction devices for heavy trucks using design of experiments and computational fluid dynamics," in *SAE*, 2005.
- [3] M. M. F. B. Mustapha Hammache, "Aerodynamic forces on truck model, including two trucks in tandem," *California Path Program*, pp. 1-25, 2001.
- [4] L. L. H. A. Thomas Curry, "Reducing aerodynamic drag and rolling resistance from heavy duty trucks: Summary of available technologies and applicability to chinese trucks.," MJ Bradley and Associates LLC, California, 2012.
- [5] Y. Z. T. Charles, "Impact of gap size between two bluff bodies on the flow", in *ASTFE*, Portoroz, 2017.
- [6] R. M. Wood, "Road transport technology," (Online). Available: <http://road-transport-technology.org/Proceedings/9%20-%20ISHVWD/Session%209/A%20Discussion%20of%20a%20Heavy%20Truck%20Advanced%20Aerodynamic%20Trailer%20System%20-%20Wood.pdf>. (Accessed 26 04 2019).
- [7] N. C. Pradeep Kumar, "Enhancement of Aerodynamic efficiency of truck-trailer," *International Journal of Innovative Research in Science, Engineering and Technology*, vol. 5, no. 6, pp. 9563 - 9573, 2016.
- [8] M. B. F. Hammache, "On the aerodynamics of tractor-trailers. In: *The Aerodynamics of Heavy Vehicles: Trucks, Busses and Trains*," Springer, Monterey, 2002.
- [9] J. Allan, "Aerodynamic drag and pressure measurements on a simplified tractor-trailer model," *Journal of Wind Engineering and Industrial Aerodynamics*, vol. 9, pp. 125-136, 1981.
- [10] S. K. Jan Osth, "The flow around a simplified tractor-trailer model studied by large eddy simulation," *Journal of Wind Engineering and Ind Aerodynamics*, vol. 102, pp. 36-47, 2012.